The influence of roughness on the resistance to impact of different CAD/CAM dental ceramics

Luis Felipe Guilardi [1], Arie Werner [2], Niek de Jager [2], Gabriel Kalil Rocha Pereira [1], Cornelis Johannes Kleverlaan [2], Marilia Pivetta Rippe [1], Luiz Felipe Valandro [1].

[1] Federal University of Santa Maria, Faculty of Dentistry, Department of Restorative Dentistry, Santa Maria, RS, Brazil.

[2] Academic Centre for Dentistry Amsterdam - ACTA, Department of Dental Materials Science, Universiteit van Amsterdam and Vrije Universiteit, Amsterdam, The Netherlands.

This study aimed to investigate the effect of surface roughness (polished vs. CAD/CAM milling simulation) on impact strength of five dental ceramics for manufacturing CAD/CAM monolithic restorations. Specimens of five ceramics (FC- feldspathic glass-ceramic; PICN- polymer-infiltrated ceramic-network; ZLS- zirconia-reinforced lithium silicate glass-ceramic; LD- lithium disilicate glass-ceramic; YZ- yttria-stabilized tetragonal zirconia polycrystal ceramic) to be tested under impact ($15 \times 10 \times 2mm^3$; n= 15) were divided into two groups, according to surface treatment: polishing (*pol*) and grinding (*gri*) as CAD/CAM milling simulation. Impact strength was tested using the Dynstat method. Roughness, topographic, fractographic and finite element analyses were performed. The impact strength data were analyzed by Weibull, and Pearson correlation was used to correlate roughness and impact strength data. The CAD/CAM milling simulation led to significantly (p<0.05) greater roughness (Ra and Rz) and statistically reduced the impact strength for PICN (*pol*PICN= 4.59 to *gri*PICN= 1.09; ±76% decrease), for LD (*pol*LD= 17.69 to *gri*LD= 10.09; ±43% decrease) and for YZ (*pol*YZ= 74.99 to *gri*YZ= 20.67; ±72% decrease) ceramics; and also promoted a more irregular topography with scratches and grooves. Fractographic and FEA analyses depicted the origin of failure at the higher stress concentration side during the impact test, where the pendulum impacted. The CAD/CAM milling simulation significantly decreased the impact strength of the evaluated ceramic materials.

Correspondence: Gabriel Kalil Rocha Pereira
Federal University of Santa Maria, Faculty of Odontology, MDS-PhD Graduate Program in Oral Science, Prosthodontics Unit.
Address: Avenue Roraima 1000, Building 26F, Room 2383, Zip-Code: 97105-900, Santa Maria, Rio Grande do Sul, Brazil. Fax: +55-55-3220-9210. E-mail: gabrielkrpereira@hotmail.com

Introduction

The use of ceramic materials for manufacturing fixed dental prostheses (FDPs) is intensely common nowadays in dental practice. The major processing technique that has been explored is through Computer-Aided Design and Computer-Aided Manufacturing (CAD/CAM) systems as they enable increased process reliability, high cost-effectiveness and a substantial reduction in working time (1).

The ceramic materials are mainly classified according to their composition (i.e. silica-based ceramics, oxide ceramics, resin-matrix ceramics) and manufacturing method (i.e. layering, pressing and CAD/CAM milling) (2). Ideally, we seek to use a material that provides adequate aesthetics, combined with high mechanical properties. Preferably, this material must withstand high loads and must resist crack propagation as much as possible (3). It is very clear that the ceramic microstructure directly influences the mechanical properties of the material, and the higher the crystalline phase content, the better the material's mechanical properties tend to be (4). However, even the most resistant dental ceramic material (e.g., yttria-stabilized tetragonal zirconia polycrystal) is prone to crack propagation, because ceramics are brittle by nature (5). New materials have sought to increase the energy absorption capacity generated at the crack tip, and thus delaying the crack propagation. One example is the polymer-infiltrated ceramic network (Vita ENAMIC®; VITA Zahnfabrik), also referred as a hybrid ceramic, that have a polymeric matrix or network structure combining organic (polymer network - 25% by volume) and inorganic (feldspathic ceramic network - 75% by volume) components (2).

Although ceramic restorations produced by machining ceramic blocks can optimize and improve the structural reliability of the material itself, the effect of the machining process on the long-term stability of these restorations must be considered. This is because CAD/CAM systems use abrasive machining processes that have a high potential to generate damage to the material's surface and subsurface, which may reduce the integrity of the final restoration (6-8). If these damages are more

severe than the pre-existing defects in the material, they assume an important role in the material resistance (6). According to Fraga et al. (7) and Romanyk et al. (8), specimens machined in CAD/CAM show evidence of damage inserted by machining in the form of lateral and radial cracks, chips, subsurface damage and residual stresses. Cracks are usually located on the periphery or exactly at the material's failure origin site (8). These damages introduced during subtractive machining limit the strength of the material and are not eliminated during crystallization (e.g., silicate and lithium disilicate-based glass ceramics), sintering (e.g., zirconia) or annealing/crack blunting (e.g., pre-crystallized lithium silicate – Celtra® Duo). In addition, the internal surface remains untouched (as milled), while the external surface of a restoration can be finished, polished and/or glazed to reduce or remove such damages (9).

In addition to the presence of intermittent cyclic loading during mastication in the oral environment, overload can occur for an intermittent period (i.e. parafunctional habit like bruxism and clenching) or abruptly (i.e. traumatic accident) and be immediately transferred to the dental structures. The involuntary parafunctional habit, the chewing of hard foods and the shock suffered in accidents can generate excessive and extreme stress to the dental structures, often causing cracks and fracture of the dental element/restoration/implant (10-12). In such scenarios, the fracture mechanism may be completely different from that considered in literature through static and fatigue tests (13,14). To the best of the authors' knowledge, the impact strength data of current CAD/CAM chairside dental ceramics are not reported in the dental literature, as well as the effect of the ceramic microstructure/characteristics and ceramic surface condition (polished vs. ground) on such mechanical property.

Therefore, understanding the nature of milling damage is an essential prerequisite for evaluating the reliability of brittle materials as structural components of an oral rehabilitation, especially during overloading episodes (e.g., parafunctional habits, shock by accidents). The present study focuses on different classes of ceramic materials supplied as CAD/CAM blocks and indicated for monolithic restorations. The ceramic materials were selected, subjected to surface treatments (polishing or grinding – to simulate the CAD/CAM milling effect) and tested under impact force. Finally, the surface topography and the failure characteristics were analyzed. The following hypotheses were tested: 1) the grinding would significantly reduce the impact strength of all materials; and 2) the type of ceramic material would significantly influence the impact strength results.

Material and methods

The main features of the materials used in this study are presented in Box 1.

Box 1 – Materials used in the study.

Ceramic Materials	Commercial Name / Manufacturer Lot number	[a] Chemical content (wt%), microstructure, and average crystal size	Fracture toughness (K_{Ic}) in $MPa.m^{0.5}$	Elastic modulus (E) in GPa
Feldspathic glass-ceramic FC	Vitablocs Mark II for Cerec® and inLab®; shade A2C, size I-14 / VITA Zahnfabrik, Bad Säckingen, Germany Lot: 56731	56–64% SiO_2, 20–23% Al_2O_3, 6–9% Na_2O, 6–8% K_2O, 0.3–0.6% CaO, 0.0–0.1% TiO_2. Average particle size = ±4 µm. Crystal size: ±15 µm [b]	1.01 [c]	E = ±45 [a]
Polymer infiltrated ceramic network PICN	VITA Enamic; 2 M2-HT EM-14 / VITA Zahnfabrik Lot: 67300	86% inorganic ceramic (58–63% SiO_2, 20–23% Al_2O_3, 9–11% Na_2O, 4–6% K_2O, 0.5–2% B_2O_3, <1% ZrO_2, <1% CaO); 14% organic polymer (UDMA-urethane dimethacrylate, TEGDMA-triethylene glycol dimethacrylate). Crystal size: ±20 µm [b]	1.28 [c]	E = ±30 [a]

Box 1 - Continuation

Ceramic Materials	Commercial Name / Manufacturer Lot number	[a] Chemical content (wt%), microstructure, and average crystal size	Fracture toughness (K_{Ic}) in MPa.m$^{0.5}$	Elastic modulus (E) in GPa
Zirconia-reinforced lithium silicate glass-ceramic ZLS	VITA Suprinity; A2-HT PC-14 / VITA Zahnfabrik Lot: 72790	56–64% SiO_2, 15–21% Li_2O, 1–4% K_2O, 3–8% P_2O_5, 1–4% Al_2O_3, 8-12% ZrO_2, 0-4% CeO_2, 0-6% Pigments. Homogeneous, fine crystalline structure. Crystal size: ±0.5 μm [a]	1.40 [c]	E = ±70 [a]
Lithium disilicate glass-ceramic LD	IPS e.max CAD for Cerec® and inLab®; LT A2 / C 16 / Ivoclar Vivadent AG, Schaan, Liechtenstein Lot: W93126	58–80% SiO_2, 11–19% Li_2O, 0–13% K_2O, 0–8% ZrO_2, 0–5% Al_2O_3. Crystal size: ±1.5 μm [a]	2.06 [c]	E = ±95 [a]
Yttria-stabilized tetragonal zirconia polycrystal ceramic YZ	VITA YZ-55/19 T White for inLab / VITA Zahnfabrik Lot: 76030	90.9–94.5% ZrO_2, 4–6% Y_2O_3, 1.5-2.5% HfO_2, 0-0.3% Al_2O_3, 0-0.3% Fe_2O_3. Crystal size: ±500 nm [a]	4.5 [a]	E = ±210 [a]

[a]As disclosed by manufacturers; [b]Belli et al. (4); [c]Lube et al. (46)

Preparation of specimens

Thirty rectangular plates were produced for each material based on the impact test configuration. For the feldspathic glass-ceramic - FC (Vitablocs Mark II), polymer-infiltrated ceramic-network - PICN (VITA Enamic), zirconia-reinforced lithium silicate ceramic - ZLS (VITA Suprinity), and lithium disilicate glass-ceramic - LD (IPS e.max CAD) groups, the specimens were cut in a high precision machine with a diamond saw (Isomet 1000, Buehler; Lake Bluff, IL, USA) under constant water cooling into their final dimensions of 15.0 × 10.0 × 2.0 mm^3. The yttria-stabilized tetragonal zirconia polycrystal - YZ (VITA YZ-55/19 T), the specimens were cut to a 20% larger (18.0 × 12.0 × 2.4 mm^3) due to shrinkage after sintering. The specimens were then polished (SiC papers #280-, #400- and #800-grit sizes) and divided into two groups according to the surface treatments, polishing and grinding, which were performed before the crystallization and sintering processes.

Surface treatment

Polishing and grinding (CAD/CAM milling simulation) protocols were standardized for all the materials, as follows:

Polishing 'pol' – a grinding machine (ECOMET Grinder/Polisher, Buehler) was used to polish the specimens with SiC papers (#1200 and #2500-grit sizes; Buehler) under constant water cooling.

Grinding (CAD/CAM milling simulation) 'gri' – the specimen was ground over a #60-grit size SiC paper (P60 - Black Stone Waterproof; BOSCH, Campinas, SP, Brazil), using light finger pressure for 30 s in oscillatory movements under constant water cooling. This same protocol was used in previous studies (13,15) to simulate the surface roughness left by the CAD/CAM milling process (9).

Next, the specimens were crystallized and sintered according to the manufacturers' instructions: ZLS (840 ºC for 8 min) and LD (840 ºC for 7 min) specimens were crystallized in a porcelain furnace (Programat P100, Ivoclar Vivadent); and YZ (1530 ºC for 120 min) specimens were sintered (Cercon Heat, Degudent GmbH, Hanau-Wolfgang, Germany). The specimens from FC and PICN materials do not require an additional firing treatment.

Roughness analysis

Six measurements (three on each axis - *x* and *y*) were performed on each specimen using a profilometer (Mitutoyo SJ-400, Mitutoyo Corporation, Japan), following the ISO 4287 (16) instructions (cut-off wavelengths= 0.8 mm (n= 5); λs= 2.5 μm). The analysis was performed after the crystallization and sintering processes and the parameters *Ra* (arithmetic mean of the absolute roughness values of the peaks and valleys measured from a medium plane) and *Rz* (average distance between the five highest peaks and five lowest valleys found in the standard) were recorded in μm.

Impact strength – Dynstat method (n= 15)

The impact strength consists in the dynamic breaking of the sample and reading the amount of energy used to break it on the scale of the apparatus. A Dynstat apparatus (Zwick & Co., Eisingeu, Germany) was used according to the ISO 13802 (17) by which an impact test can be performed, where a flat pendulum is dropped to impact on the specimen that was fixed in a jig. The principle of the impact strength test is schematically drawn in Figure 1. Corrected absorbed energy (E_c) was recorded, and the impact strength of each specimen was calculated according to the following formula:

The impact strength (a_{cU}) was calculated in kilojoules per square meter (kJ/m^2) using equation 1

$$a_{cU} = \frac{E_c}{hb} \times 10^3 \qquad \text{Eq. (1)}$$

where E_c is the corrected energy absorbed by breaking the test specimen [J], *h* is the height and *b* is the width of the specimen [mm].
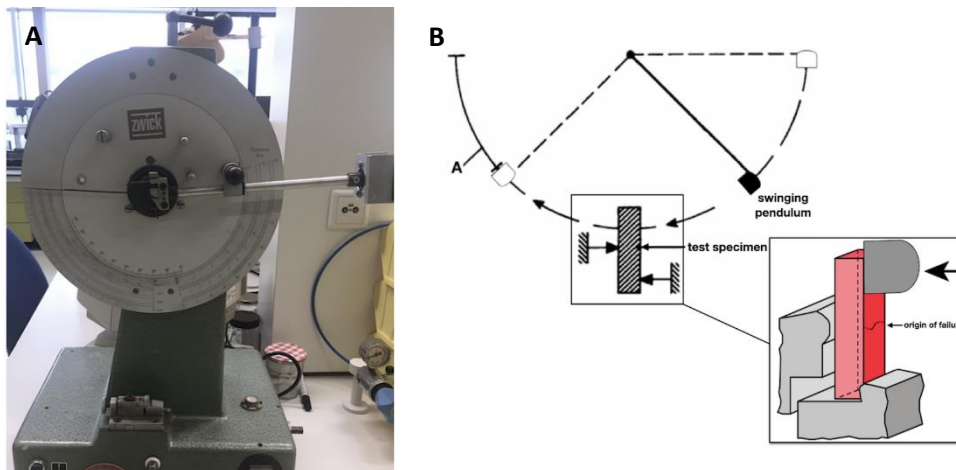

Figure 1. Impact test assembly. A) Dynstat apparatus for determination of impact strength, and B) principle of impact strength test: arc-length A is proportional to energy absorbed by breaking of the specimen. Design adapted from de Wijn et al. (45) and Zwick/Roell Group for Dynstat test.

Topographic analysis

Surface topographic images were taken from all groups in polished and ground conditions to determine their topographic pattern. Representative specimens (n= 2) were cleaned with isopropyl alcohol for 10 minutes in an ultrasonic cleaner (1440 D, 50/60 Hz, Odontobras, Ribeirao Preto, SP, Brazil), dried with air spray, gold sputtered and analyzed at 100× magnification by Scanning Electron Microscope – SEM (XL 20, FEI Company, Eindhoven, The Netherlands).

Fractographic analysis

After the impact test, the specimens were evaluated in stereomicroscope (Olympus, Shinjuku, Tokyo, Japan) at 100× magnification. Representative specimens were selected, ultrasonically cleaned (1440 D, 50/60 Hz, Odontobras) in isopropyl alcohol for 10 minutes, dried with air spray, gold sputtered, and subjected to SEM analysis (XL 20, FEI Company) at 90× magnification.

Finite Element Analysis – FEA

A simplified three-dimensional FEA model of the impact test set-up with the same dimensions as the test set-up was created. The model consisted of the direct environment of the test sample of the impact tester supports and the part of the hammer in contact with the test sample, and the test sample itself. The surfaces in the interface between the impact tester and the test material were modeled with contact surfaces with a friction coefficient of 0.45. The Finite Element modeling was carried out using FEMAP software (FEMAP 11.1.2; Siemens PLM software, Plano, TX, USA), while the analysis was done with NX Nastran software (NX Nastran; Siemens PLM Software, Plano, TX, USA). For the dimensions of the specimen, see Figure 2. The model was composed of 30,952 parabolic tetrahedron solid elements. The mechanical properties of the materials of the test samples used were based on previous studies (Box 1) and the support and the hammer were made of steel (E= 200 GPa; Poisson ratio= 0.3). The investigated materials are supposed to have brittle behavior in the impact test, so the deformation is linear to the load to failure. The kinetic energy of the pendulum in the impact tester is transferred into displacement energy of the test sample at the point of contact with the pendulum. Therefore, the impact on the test sample can be represented as a static force. A load of 100 N was applied on the hammer back surface. The nodes at the bottom of the impact tester were fixed and the nodes at the bottom of the pendulum were allowed to slide along the surface only.
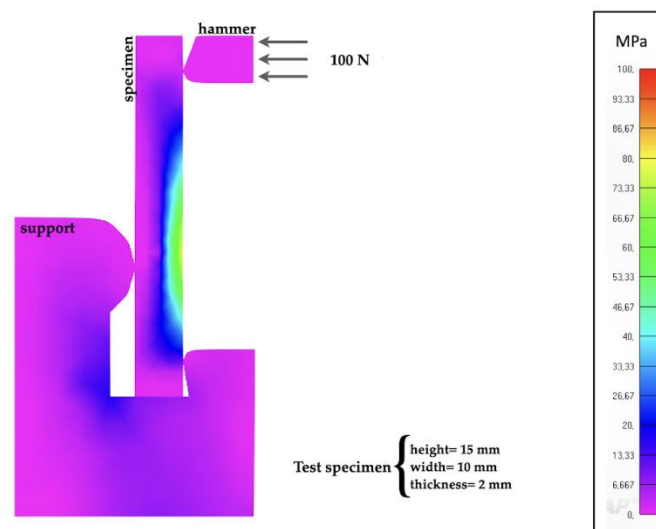

Figure 2. Representative image of FEA analysis showing the maximum principal stress concentration at the surface when the pendulum impacts the specimen (polished feldspathic ceramic) during the impact test. This analysis was used to illustrate where it concentrates the maximum principal stress in such test, which is few applied in dental ceramic studies.

Statistical analysis

SPSS v.23.0 (SPSS IBM, Chicago, IL, USA) was used to execute statistical tests with $\alpha= 0.05$. Roughness data were analyzed with the parametric tests Two-way ANOVA and Tukey's HSD (Honestly Significant Difference) post-hoc. A Pearson correlation analysis was run for all the ceramic materials to identify linear correlations between the roughness (Ra) and the impact strength parameters. A Pearson correlation is a number between -1 and +1 that indicates the extent to which two variables are linearly related. The variables may be perfectly negatively (-1) or positively (+1) linearly related, or they don't have any linear relation whatsoever (0). According to Cohen (18), a correlation intensity between 0.10 and 0.29 are considered a weak correlation, 0.30 to 0.49 as medium, and 0.50 to 1.00 is considered a high correlation.

The impact test data were analyzed through Weibull analysis (19) using the SuperSMITH Weibull 4.0k-32 software (Wes Fulton, Torrance, CA, USA) in order to determine the characteristic strength (σ_0 – strength at a failure probability of approximately 63%) and the Weibull modulus (expresses the mechanical reliability of the material) of the groups. The Weibull plot has the 95% confidence bounds of the estimate for the Weibull shape parameter (Weibull modulus, m) on the Y-axis, and 95% confidence

bounds for the estimate of the characteristic strength (σ_o) on the X-axis. If contour plots intersect, Weibull parameters are not statistically different (20).

Results

The specimens subjected to CAD/CAM milling simulation had a rougher surface (*Ra* and *Rz*) compared to polished ones for all the materials (Table 1).

Table 1 – Impact test data: roughness (Ra and Rz); Pearson correlation coefficient (R) between *Ra* and impact strength; Weibull analysis (Mean and 95% Confidence Interval - CI); and the decrease of 'σ_{olt}' from polished to CAD/CAM milling simulation condition.

Study Groups	[†] Roughness (μm) Mean (standard deviation – SD)		R (p value)	[f] Weibull Analysis Mean (95% Confidence Interval – CI)		σ_{olt} decrease from p/gr
	Ra	*Rz*	σ_{olt} × *Ra*	Characteristic strength σ_{olt} (kJ/m²)	Weibull modulus (*m*)	
*pol*FC	0.14 (0.02) [E]	0.80 (0.08) [F]	−0.15 (0.42)	0.83 (0.72– 0.94) [F]	4.10 (2.86 – 5.87) [AB]	±13%
*gri*FC	1.12 (0.12) [D]	4.67 (0.43) [E]		0.72 (0.62– 0.83) [F]	4.26 (3.61 – 5.02) [AB]	
*pol*PICN	0.06 (0.01) [E]	0.59 (0.10) [F]	−0.92 (0.00)	4.59 (4.09 – 5.16) [D]	4.65 (3.00 – 7.20) [AB]	±76%
*gri*PICN	2.36 (0.23) [B]	13.77 (1.32) [B]		1.09 (0.98 – 1.23) [E]	4.67 (3.15 – 6.92) [AB]	
*pol*ZLS	0.04 (0.00) [E]	0.52 (0.06) [F]	−0.53 (0.00)	16.51 (12.18 – 22.38) [BC]	1.80 (1.13 – 2.86) [C]	±37%
*gri*ZLS	1.70 (1.11) [C]	10.71 (0.15) [C]		10.37 (8.50 – 12.65) [C]	2.77 (1.73 – 4.42) [BC]	
*pol*LD	0.05 (0.01) [E]	0.46 (0.08) [F]	−0.61 (0.00)	17.69 (14.91 – 20.98) [B]	3.10 (2.05 – 4.68) [ABC]	±43%
*gri*LD	1.58 (0.16) [C]	9.42 (0.88) [D]		10.09 (9.30 – 10.95) [C]	6.55 (4.43 – 9.67) [A]	
*pol*YZ	0.12 (0.01) [E]	1.04 (0.10) [F]	−0.83 (0.00)	74.99 (63.29 – 88.85) [A]	3.20 (2.04 – 4.99) [ABC]	±72%
*gri*YZ	3.80 (0.50) [A]	21.05 (2.32) [A]		20.67 (17.57 – 24.31) [B]	3.62 (2.98 – 4.40) [B]	

Different uppercase letters in each column indicate statistically significant difference based on the [†] Two-Way ANOVA and Tukey's HSD Post-hoc, and based on the [f] Confidence Intervals overlapping of the Weibull analysis.

For the impact strength data, FC showed the lowest values, followed by PICN, LD and ZLS presented intermediary results, and YZ the highest results (Table 1). The characteristic strength of the impact test results was statistically reduced after the CAD/CAM milling sim for PICN (76% of decrease), LD (43%) and YZ (72%) ceramics (Table 1). The Weibull modulus did not differ within each type of ceramic (Table 1).

The Pearson Correlation analysis show a high and negative Pearson correlation coefficient for PICN, ZLS, LD and YZ materials, and no correlation for FC (Table 1).

SEM topographic images clearly show a more irregular surface for the materials in the ground condition, presenting scratches and grooves along the surface. In addition, differences between the groups submitted to CAD/CAM milling simulation highlight their different behavior due to their distinct physical and mechanical characteristics (Figure 3). In the Feldspathic Ceramic surface, it is possible to observe inherent defects (bubbles and fissures) of the material, since these remained after high polishing (Figure 3A).

The fractographic analysis of the impact test specimens (Figure 4) shows the failure origin located at the principal stress concentration region in the impact strength test, according to the FEA analysis showed in the Figure 2.

The FEA analysis showed that the maximum principal stress concentrates at the surface when the pendulum impacts the specimen at the height of the support, for all the materials, as demonstrated by the representative image in Figure 2.
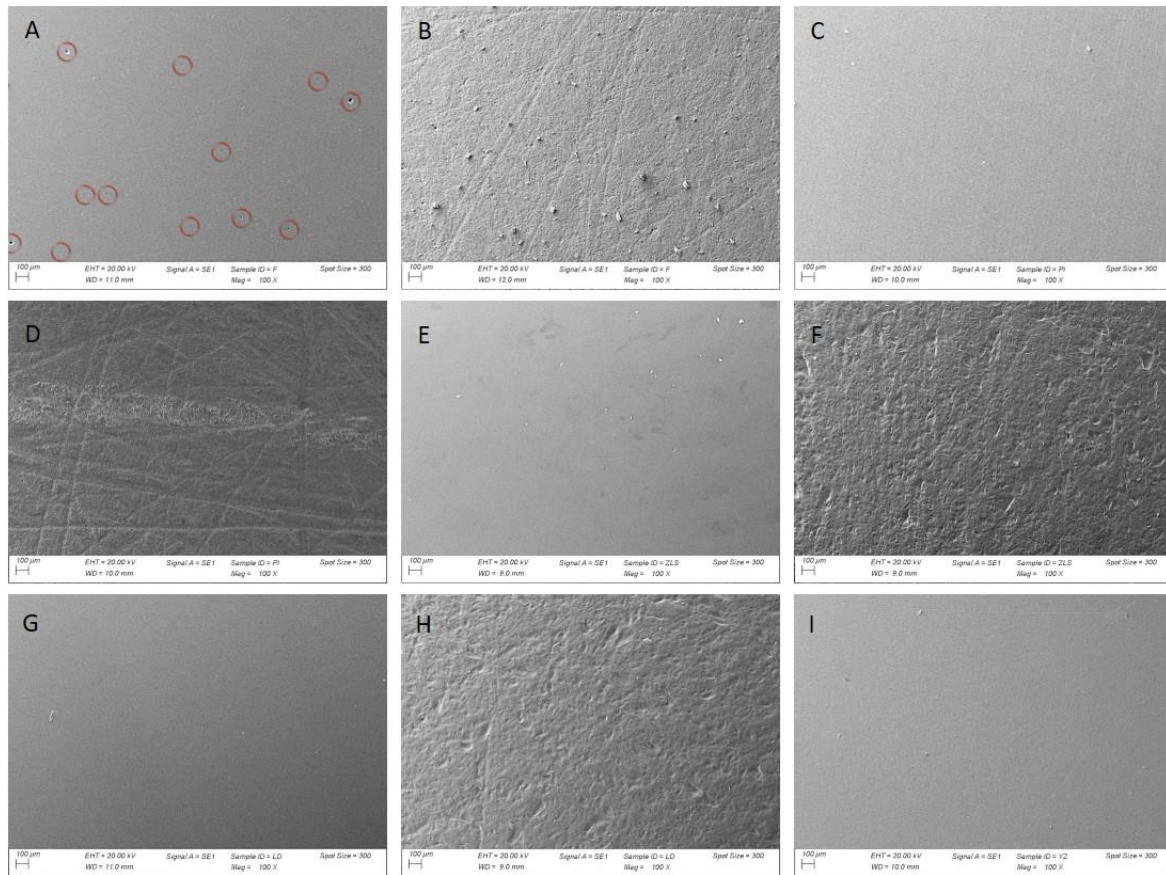
Figure 3. SEM images (100× of magnification) of the ceramics' surfaces on polished and ground conditions. On the FC polished condition, the red circles point to the defects (e.g., fissures and bubbles) that remained after the polishing protocol being applied.
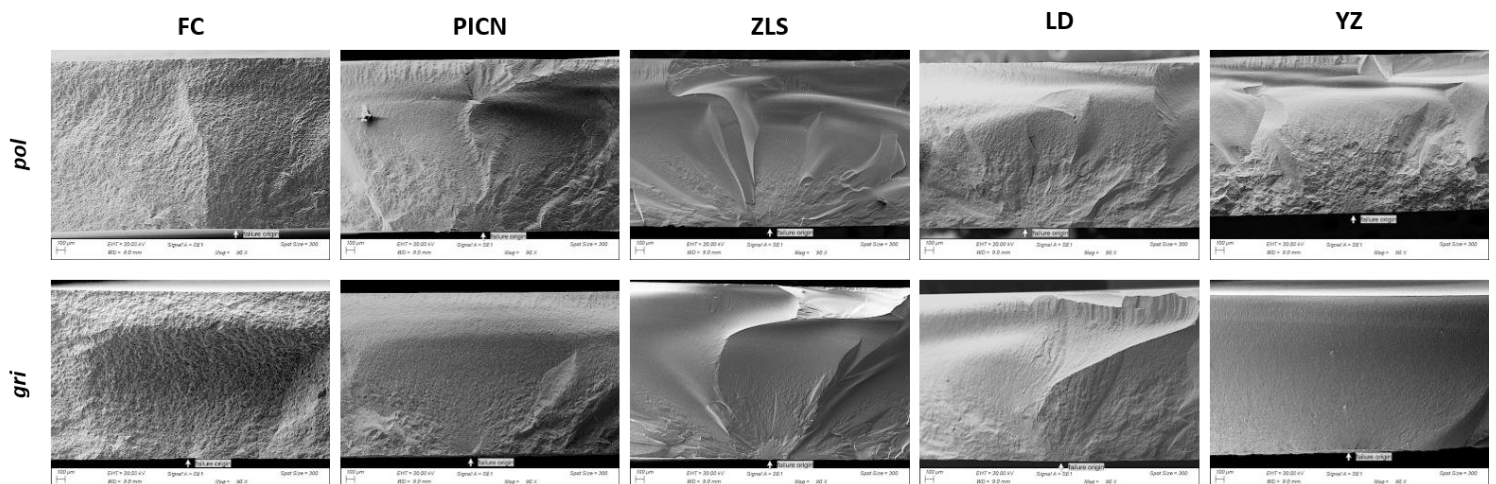

Figure 4. Fractographic images (90× of magnification) on SEM of the groups in the polished and ground conditions, showing the typical fractographic characteristics after the impact strength test. The origin of failure corresponds to the region of maximum tensile stress in the impact strength test, according to the FEA analysis in the Fig. 2.

Discussion

The dental literature has shown that the optical and mechanical characteristics of ceramic materials are related to their composition, microstructure, and surface state (4,13,21-24). Such a relationship was also found in our study, where the different materials and surface conditions provided distinct results from the impact test. Thus, the study's hypotheses had to be accepted by the authors.

The grinding process, used to simulate the CAD/CAM milling effect on the ceramic surface, significantly increased the roughness of the materials, and consequently reduced their resistance to the impact force (Table 1). In general, a rougher surface leads to a drop in the mechanical resistance of the studied ceramics (13,25). Although the roughness created by CAD/CAM milling has an initial negative effect on the nominal strength of the ceramic materials (7,9), we should consider that the ceramic surfaces, inner and outer surfaces, will be treated (e.g., glazing, polishing, hydrofluoric acid etching, air-abrasion) prior to its adhesive bonding to the substrate (26), which in turn will change its topographical pattern (26,27). The inner ceramic surface is the most exposed to the milling-generated surface and subsurface damages, since it does not receive any treatment (e.g., polishing or glazing) capable of reducing the length of the critical surface defects (7,9,28,29). But if these defects are properly filled by the bonding system, the strength and the structural reliability of the material may be restored (30-33).

The purpose of the impact test is to ascertain the behavior of specified test specimens under defined impact loading conditions, and to assess the material's flexural strength based on the impact strength results. The swinging pendulum (Fig. 1B) first measures the energy required to break a specimen and then the strength is calculated. As demonstrated by Brostow and Lobland (34), the impact strength is connected to the material brittleness, and as the machining process introduces defects on the ceramic surface, its surface roughness increases, in turn jeopardizing its biaxial flexural strength (9). The characteristic strength from the impact data was statistically significant reduced for PICN (76% of decrease), LD (43%) and YZ (72%) ceramics after they were submitted to the CAD/CAM milling simulation, and the Weibull modulus remained statistically equal between polishing and grinding conditions, within each type of ceramic (Table 1). It is important to highlight that the polished YZ material presented impact strength results much higher than the other materials. However, we must consider that the YZ impact strength was reduced to the level of the polished ZLS and LD materials after the CAD/CAM milling simulation (Table 1). In this sense, the clinicians may be concerned that for such material the surface roughness should be more detrimental in terms of resistance to impact forces.

During the contact between the diamond drill and the ceramic surface, a concentration of localized stress occurs, resulting in microfracture and loss of material, which varies according to the characteristics of the ceramic material (6). The dynamics of the grinding that occurs in the ceramic generates effects on the surface and subsurface of the material, creating medial and lateral cracks (8). The interaction between the strength-limiting cracks and the created residual stress field can determine the final strength of the ceramic material (6). The mechanical response of the studied materials is different due to their different composition and characteristics. As stated by Bloyer et al. (35), the amount and composition of the glass phase on the ceramic microstructure strongly influences its mechanical properties. Based on the ceramics' crystalline content, the literature has shown that generally the greater crystalline content, the greater the material capacity to resist the static and fatigue loading (4,21,23). Both glass phase and crystalline content are responsible for the material toughening mechanisms, which controls the crack growth in ceramics, and by that is directly related to the material strength (24). According to Kruzic et al. (24), the microstructural differences between the ceramic materials make them behave differently to the crack growth. PICN material for example has the crack bridging and the plastic deformation zone around the crack tip acting as toughening mechanisms; the particle-reinforced glass-ceramics (FC, LD and ZLS) have the crack deflection mechanism; and the polycrystalline ceramic (YZ) has the toughening mechanism due to phase-transformation (24). Such notes are corroborated by the findings of our study, in which the material with less glass phase, more crystalline content, and higher toughness (YZ) presented better resistance to the impact test, and so on for the other materials studied (ZLS and LD > PICN > FC) (Box 1 and 2).

The Pearson's linear correlation coefficient demonstrated a high negative linear correlation for the materials, meaning that as the material's roughness increases, the resistance to impact force decreases. The exception was the feldspathic ceramic, which showed no correlation between the roughness values and the impact strength. Such difference may be due to the small variation in the roughness values between the polished (*pol*FC) and ground (*gri*FC) conditions (Tables 2). Also, the presence of intrinsic flaws in this ceramic material (microstructural heterogeneities and pores; indicated by red circles in Fig. 3A), even after polishing, may have reduced the effect of superficial defects created by the CAD/CAM

milling simulation protocol. The presence of internal defects may determine the strength of the material (36,37). According to the fracture analysis performed by Quinn et al. (38) in a feldspathic ceramic, the intrinsic flaws present in this material could be the nature of strength-limiting defects, and the polishing would be unable to remove such defects. The Griffith's law (39) and the slow crack growth mechanism (40) may help to explain this phenomenon, as the presence of critical defects can lead to damage accumulation, jeopardizing the nominal strength of the material. Griffith stated that the strength of a solid elastic body is governed by the presence of microscopic flaws (39). Since the stress field concentrates more around critical flaws, the energy required to break the material at this site is reduced.

The topographic analysis, besides showing intrinsic flaws at the FC material, issue discussed above, shows that the grinding process created a more irregular surface (scratches, pits, and fissures) in all the material (Fig. 3). One can easily observe the differences between the materials surfaces in their respective ground - CAD/CAM milling simulation - groups, even they have been submitted to the same grinding protocol. The fractographic analysis of the broken specimens shows that the failure origin is located at the main region of stress concentration during testing (Fig. 4), being in accordance with the FEA analysis (Fig. 2) and with the study of Thomaidis et al. (41), corresponding to the tensile tension side, in which the pendulum strikes the specimen.

Once the CAD/CAM milling creates surface alterations to the ceramics' surface and subsurface (i.e. residual stresses, lateral/median cracks, chippings, among others) (6,8,42-44), the authors consider that the use of CAD/CAM-milled specimens would have been the best option for the study. This approach was not possible due to a cost limit. Even not exactly mimicking the effects of CAD/CAM, the protocol used allowed for a standardization of grinding on the different ceramic materials, making the study results directly linked to the materials compositions. In addition, the use of cemented specimens would bring a broader and more related response to the impact failure mechanism eventually suffered by the patient, since bonding changes the stress distribution along the restorative set (33). Thus, further studies evaluating the impact resistance of different dental ceramics using adhesively bonded CAD/CAM milled specimens, would bring data closer to clinical findings. Also, the variables from different CAD/CAM systems and brands (i.e. size of diamond particles on the burs, number of burs, rotation speed, coolant liquid, age and number of milling procedures performed by the burs before milling a new block) may have different impact on the ceramics (8,40-42) and they should be considered in future studies.

Within the limitations of this in vitro study, it can be concluded that the characteristics of the ceramic materials determine their mechanical properties, and the higher the crystalline content, the greater the impact strength. Also, the impact strength of PICN, LD and YZ ceramic materials was statistically significant reduced after the CAD/CAM milling simulation, but the reliability of the materials was not influenced by the surface treatment.

Declaration of competing interes

The authors declare there is no conflict of interest.

Resumo

Este estudo teve como objetivo investigar o efeito da rugosidade da superfície (polido vs. simulação da usinagem em CAD/CAM) na resistência ao impacto de cinco cerâmicas odontológicas indicadas na fabricação de restaurações monolíticas em CAD/CAM. Espécimes de cinco cerâmicas (FC- vitrocerâmica

feldspática; PICN- rede de cerâmica infiltrada com polímero; ZLS- vitrocerâmica de silicato de lítio reforçada com zircônia; LD- vitrocerâmica de dissilicato de lítio; YZ- cerâmica policristalina de zircônia tetragonal estabilizada com ítria), a serem testados sob impacto ($15 \times 10 \times 2mm^3$; n= 15), foram divididos em dois grupos, de acordo com o tratamento superficial: polimento (*pol*) e desgaste (*gri*), usado como simulação da usinagem em CAD/CAM. A resistência ao impacto foi testada usando o método Dynstat. Foram realizadas as análises de rugosidade, topografia, fractografia e análise de elementos finitos. Os dados de resistência ao impacto foram analisados pela análise de Weibull, e a correlação de Pearson foi usada para correlacionar os dados de rugosidade e resistência ao impacto. A simulação da usinagem em CAD/CAM levou a uma rugosidade (Ra e Rz) significativamente maior ($p < 0,05$) para todas as cerâmicas, e reduziu estatisticamente a resistência ao impacto para as cerâmicas PICN (*pol*PICN = 4,59 para *gri*PICN = 1,09; redução de ± 76%), LD (*pol*LD = 17,69 para *gri*LD = 10,09; ± 43% de redução) e YZ (*pol*YZ = 74,99 para *gri*YZ = 20,67; ± 72% de redução); e também promoveu uma topografia mais irregular apresentando riscos e sulcos acentuados. As análises de fractografia e de elementos finitos mostraram a origem da falha no lado de maior concentração de tensão durante o teste de impacto, onde o pêndulo impactou o espécime. A simulação da usinagem em CAD/CAM reduziu significativamente a resistência ao impacto dos materiais cerâmicos avaliados.

References

1. Miyazaki T, Hotta Y, Kunii J, Kuriyama S, Tamaki Y. A review of dental CAD/CAM: current status and future perspectives from 20 years of experience. Dent Mater J 2009;28(1):44-56.

2. Gracis S, Thompson VP, Ferencz JL, Silva NR, Bonfante EA. A new classification system for all-ceramic and ceramic-like restorative materials. Int J Prosthodont 2015;28:227–235.

3. Zhang Y, Kelly JR. Dental ceramics for restoration and metal veneering. Dent Clin North Am 2017;61(4):797–819.

4. Belli R, Wendler M, de Ligny D, Cicconi MR, Petschelt A, Peterlik H, et. al. Chairside CAD/CAM materials. Part 1: Measurement of elastic constants and microstructural characterization. Dent Mater 2017;33(1):84–98.

5. Denry I, Holloway JA. Ceramics for dental applications: A review. Materials (Basel) 2010;3(1):351-68.

6. Marshall DB, Evans AG, Khuri Yakub BT, Tien JW, Kino GS, 1983. The nature of machining damage in brittle materials. Proc R Soc Lond A 1983;385:461–475.

7. Fraga S, Amaral M, Bottino MA, Valandro LF, Kleverlaan CJ, May LG. Impact of machining on the flexural fatigue strength of glass and polycrystalline CAD/CAM ceramics. Dent Mater 2017;33(11):1286-97.

8. Romanyk DL, Martinez YT, Veldhuis S, Rae N, Guo Y, Sirovica S, Fleming GJP, Addison O. Strength-limiting damage in lithium silicate glass-ceramics associated with CAD-CAM. Dent Mater 2019;35:98-104.

9. Fraga S, Valandro LF, Bottino MA, May LG. Hard machining, glaze firing and hydrofluoric acid etching: Do these procedures affect the flexural strength of a leucite glass-ceramic? Dent Mater 2015;31(7):e131-40.

10. Silva NR, Nourian P, Coelho PG, Rekow ED, Thompson VP. Impact fracture resistance of two titanium-abutment systems versus a single-piece ceramic implant. Clin Implant Dent Relat Res 2011;13(2):168-73.

11. Andersson L. Epidemiology of traumatic dental injuries. J Endod 2013;39(3Suppl):S2-5.

12. Zaleckiene V, Peciuliene V, Brukiene V, Drukteinis S. Traumatic dental injuries: etiology, prevalence and possible outcomes. Stomatologija 2014;16(1):7-14.

13. Rodrigues CDS, Guilardi LF, Follak AC, Prochnow C, May LG, Valandro LF. Internal adjustments decrease the fatigue failure load of bonded simplified lithium disilicate restorations. Dent Mater 2018;34(9):e225-235.

14. Wendler M, Belli R, Valladares D, Petschelt A, Lohbauer U. Chairside CAD/CAM materials. Part 3: Cyclic fatigue parameters and lifetime predictions. Dent Mater 2018;34:910-921.

15. Guilardi LF, Soares P, Werner A, de Jager N, Pereira GKR, Kleverlaan CJ, Rippe MP, Valandro LF. Fatigue performance of distinct CAD/CAM dental ceramics. J Mech Behav Biomed Mater 2020a;103:103540.

16. ISO 4287. Geometrical product specifications (GPS) – surface texture: profile method, terms definitions and surface texture parameters. Geneva: International Organization for Standardization; 1997.

17. ISO 13802. Plastics – Verification of pendulum impact-testing machines – Charpy, Izod and tensile impact-testing. 2nd ed. Switzerland: Geneva; 2015.

18. Cohen, Jacob. (1988), Statistical power analysis for the behavioral sciences. Hillsdale, NJ, Erlbaum.

19. Weibull W. A statistical distribution function of wide applicability. J Appl Mech 1951;18:293-297.

20. Ramadhan A, Thompson GA, Maroulakos G, Berzins D. Analysis of flexural strength and contact pressure after simulated chairside adjustment of pressed lithium disilicate glass-ceramic. J Prosthet Dent 2018;120(3):439-446.

21. Ramos Nde C, Campos TM, Paz IS, Machado JP, Bottino MA, Cesar PF, et al. Microstructure characterization and SCG of newly engineered dental ceramics. Dent Mater 2016;32(7):870-878.

22. Della Bona A, Nogueira AD, Pecho OE. Optical properties of CAD-CAM ceramic systems. J Dent 2014;42(9):1202-1209.

23. Wendler M, Belli R, Petschelt A, Mevec D, Harrer W, Lube T, et al. Chairside CAD/CAM materials. Part 2: Flexural strength testing. Dent Mater 2017;33(1):99-109.

24. Kruzic JJ, Arsecularatne JA, Tanaka CB, Hoffman MJ, Cesar PF. Recent advances in understanding the fatigue and wear behavior of dental composites and ceramics. J Mech Behav Biomed Mater 2018;88:504-533.

25. Coldea A, Fischer J, Swain MV, Thiel N. Damage tolerance of indirect restorative materials (including PICN) after simulated bur adjustments. Dent Mater 2015;31(6):684-694.

26. Strasser T, Preis V, Behr M, Rosentritt M. Roughness, surface energy, and superficial damages of CAD/CAM materials after surface treatment. Clin Oral Investig 2018;22:2787-2797.

27. Guilardi LF, Pereira G, Vallau AS, Silva IA, Giordani JC, Valandro LF, Rippe MP. Fatigue failure load of a bonded simplified monolithic feldspathic ceramic: influence of hydrofluoric acid etching and thermocycling. Oper Dent 2020b;45:E21-E31.

28. Isgró G, Addison O, Fleming GJP. Transient and residual stresses in a pressable glass-ceramic before and after resin-cement coating determined using profilometry. J Dent 2011;39:368–75.

29. Isgrò G, Rodi D, Sachs A, Hashimoto M. Modulus of Elasticity of Two Ceramic Materials and Stress-Inducing Mechanical Deformation following Fabrication Techniques and Adhesive Cementation Procedures of a Dental Ceramic. Int J Biomater 2019:4325845.

30. Addison O, Marquis PM, Fleming GJ. Quantifying the strength of a resin-coated dental ceramic. J Dent Res 2008;87(6):542-547.

31. Yi YJ, Kelly JR. Failure responses of a dental porcelain having three surface treatments under three stressing conditions. Dent Mater 2011;27(12):1252-1258.

32. Spazzin AO, Guarda GB, Oliveira-Ogliari A, Leal FB, Correr-Sobrinho L, Moraes RR. Strengthening of porcelain provided by resin cements and flowable composites. Oper Dent 2016;41(2):179-88.

33. de Kok P, Pereira GKR, Fraga S, de Jager N, Venturini AB, Kleverlaan CJ. The effect of internal roughness and bonding on the fracture resistance and structural reliability of lithium disilicate ceramic. Dent Mater 2017;33(12):1416-25.

34. Brostow W; Lobland HEH. Brittleness of materials: implications for composites and a relation to impact strength. J Mater Sci 2010;45(1):242-250.

35. Bloyer DR, McNaney JM, Cannon RM, Saiz E, Tomsia AP, Ritchie RO. Stress-corrosion crack growth of Si-Na-K-Mg-Ca-P-O bioactive glasses in simulated human physiological environment. Biomaterials 2007;28:4901-4911.

36. de Jager N, Feilzer AJ, Davidson CL. The influence of surface roughness on porcelain strength. Dent Mater 2000;16(6):381-388.

37. Fischer H, Schäfer M, Marx R. Effect of surface roughness on flexural strength of veneer ceramics. J Dent Res 2003;82:972-975.

38. Quinn GD, Hoffman K, Quinn JB. Strength and fracture origins of a feldspathic porcelain. Dent Mater 2012;28(5):502-11.

39. Griffith AA. The phenomena of rupture and flow in solids. Philos Trans R Soc Lond 1921;221:163–98.

40. Gonzaga CC, Cesar PF, Miranda WG, Yoshimura HN. Slow crack growth and reliability of dental ceramics. Dent. Mater 2011;27, 394–406. https://doi.org/10.1016/j.dental.2010.10.025.

41. Thomaidis S, Kakaboura A, Mueller WD, Zinelis S. Mechanical properties of contemporary composite resins and their interrelations. Dent Mater 2013;29(8):e132-41.

42. Corazza PH, de Castro HL, Feitosa SA, Kimpara ET, Della Bona A. Influence of CAD-CAM diamond bur deterioration on surface roughness and maximum failure load of Y-TZP-based restorations. Am J Dent 2015;28(2):95-9.

43. Curran P, Cattani-Lorente M, Anselm Wiskott HW, Durual S, Scherrer SS. Grinding damage assessment for CAD-CAM restorative materials. Dent Mater 2017;33(3):294-308.

44. Madruga CFL, Bueno MG, Dal Piva AMO, Prochnow C, Pereira GKR, Bottino MA, Valandro LF, de Melo RM. Sequential usage of diamond bur for CAD/CAM milling: Effect on the roughness, topography and fatigue strength of lithium disilicate glass ceramic. J Mech Behav Biomed Mater 2019;91:326-334.

45. de Wijn JR, Slooff TJ, Driessens FC. Characterization of bone cements. Acta Orthop Scand 1975 Apr;46(1):38-51.

46. Lube T, Rasche S, Nindhia TGT. A fracture toughness test using the ball-on-three-balls test. J Am Ceram Soc 2016;99:249-256.